

On the Study of Weighted Fractional Cumulative Residual Inaccuracy and its Dynamical Version with Applications

Aman Pandey Chanchal Kundu^{a1}
Department of Mathematical Sciences
Rajiv Gandhi Institute of Technology
Jais, Raebareli, 229304

Abstract

In recent years, there has been a growing interest in information measures that quantify inaccuracy and uncertainty in systems. In this paper, we introduce a novel concept called the Weighted Fractional Cumulative Residual Inaccuracy (WFCRI). We develop several fundamental properties of WFCRI and establish important bounds that reveal its analytical behavior. Further, we examine the behavior of WFCRI under a mixture hazard model. A dynamic version of WFCRI also proposed and studied its behavior under proportional hazard rate model. An empirical estimation method for WFCRI under the proportional hazard rate model framework is also proposed, and its performance is evaluated through simulation studies. Finally, we demonstrate the utility of WFCRI measure in characterizing chaotic dynamics by applying it to the Ricker and cubic maps. The proposed measure is also applied to real data to assess the uncertainty.

Keywords: Weighted fractional cumulative residual inaccuracy; Fractional residual entropy; Proportional hazard model; Empirical estimation

Mathematics Subject Classification (2020): 62B10, 62H05, 94A17.

1 Introduction

Shannon entropy, introduced by Shannon (1948), quantifies the uncertainty in a RV and serves as a foundational concept in information theory. Let $p(w)$ be the probability distribution function of a discrete random variable (RV) X , the entropy is defined as

$$H(X) = - \sum p(w) \log p(w). \quad (1.1)$$

The entropy measures play a central role in data compression, communication theory, and statistical learning (MacKay, 2003). Beyond engineering, Shannon entropy has found applications across various fields, from physics to neuroscience, underscoring its versatility in quantifying uncertainty and information.

Rao et al. (2004) introduced an alternative measure of entropy called cumulative residual entropy of a absolutely continuous non-negative RV X as

$$\bar{H}(X) = - \int_0^{+\infty} S_X(w) \log S_X(w) dw, \quad (1.2)$$

where $S_X(\cdot) = 1 - F_X(\cdot)$ is the SF (SF) and F is the CDF of the RV X . While Shannon entropy is inherently additive, this property may not be desirable in contexts involving nonextensive systems, long-range interactions, or multifractality. To address such limitations, researchers have developed various generalizations, including the one-parameter families of Tsallis (Tsallis, 1988) and Rényi (Rényi, 1961) entropies. Among such developments, Ubriaco (2009) introduced a novel entropy measure termed fractional entropy, defined as

$$H_\alpha(X) = \sum_{i=1}^n p_i (\log p_i)^\alpha, \quad 0 \leq \alpha \leq 1. \quad (1.3)$$

This measure retains positivity and concavity, but it is generally non-additive. Notably, it reduces to Shannon entropy when $\alpha = 1$. Fractional entropy captures a nonlinear weighting of event probabilities, offering a flexible tool for modeling complex uncertainty. Machado (2014) demonstrated that fractional entropy exhibits greater sensitivity to signal evolution, enabling the extraction of more detailed information about the underlying system compared to a single entropy measure.

Building upon this idea, Xiong et al. (2019) proposed the fractional cumulative residual entropy (FCRE) for the non-negative absolutely continuous RV X , defined as

$$H_\beta(X) = \int_0^{+\infty} S_X(w) (-\log S_X(w))^\beta dw, \quad 0 \leq \beta \leq 1, \quad (1.4)$$

which generalizes the CRE by incorporating a fractional power of the information function. The authors established theoretical properties, bounds, and a consistent empirical estimator. They also examined connections between FCRE, CRE and differential entropy and derived a central limit theorem for the exponential distribution case. Applications were demonstrated in both simulated and real-world datasets.

Alomani and Kayid defied the weighted generalized FCRI. Suppose X and Y are two RVs then generalized weighted fractional cumulative residual inaccuracy (GWFCRI) is defined as

$$H_\beta^w(X) = H_\beta(X) = \frac{1}{\Gamma(\beta + 1)} \int_0^{+\infty} \Psi(w) S_X(w) (-\log S_X(w))^\beta dw, \quad \beta \geq 0.$$

Analogously weighted fractional cumulative residual entropy (WFCRE) can be defined as

$$H_\beta^w(X) = H_\beta(X) = \int_0^{+\infty} \Psi(w) S_X(w) (-\log S_X(w))^\beta dw, \quad \beta \geq 0. \quad (1.5)$$

A significant direction of recent research involves incorporating comparative distributions into entropy-based measures. Kerridge (1961) introduced the concept of the residual inaccuracy measure to assess the mismatch between the actual and hypothesized distributions, particularly in the tail region. This measure is defined as

$$\mathcal{K}(X, Y) = - \int f(w) \log g(w) dw, \quad (1.6)$$

where $f(\cdot)$ and $g(\cdot)$ represent the pdfs of true and assumed distributions, respectively. It is especially relevant in statistical inference and reliability analysis when the true model is not precisely known. The inaccuracy measure helps quantify how closely a proposed model $g(x)$ aligns with the actual data-generating process $f(x)$. Metrics like Kerridge's inaccuracy and Shannon entropy are essential tools for assessing model performance. Their theoretical foundations and applications have been extensively explored in areas such as information and coding theory, as seen in the works of Nath (1968) and Bhatia (1995). More recent developments in the study of inaccuracy measures can be found in the literature by Kundu and Nanda (2015), Kundu et al. (2016), Kayal et al. (2017), Kharazmi et al. (2024) and Kharazmi and Contreras-Reyes (2024). Additionally, Kumar and Taneja (2015) introduced a cumulative version of the inaccuracy measure, expressed as

$$K(X, Y) = - \int_0^{+\infty} S_X(w) \log S_Y(w) dw, \quad (1.7)$$

where $S_X(\cdot)$ and $S_Y(\cdot)$ denote the SFs of actual and assumed models, offering a tail-focused perspective on model discrepancy. Further, Rao et al. (2005) studied CRE and they established several theoretical properties of CRE, highlighting its advantages over Shannon entropy. The paper also demonstrated CRE's potential through applications in reliability engineering and computer vision.

More recently, Kharazmi and Contreras-Reyes (2024) introduced the fractional cumulative residual inaccuracy (FCRI) measure, an extension of the FCRE to a two-distribution setup. For RVs X and Y with SFs $S_X(w)$ and $S_Y(w)$, respectively, the FCRI is defined as

$$\mathcal{K}_\beta(S, S_Y) = \int_0^{+\infty} S_X(w) (-\log S_Y(w))^\beta dw. \quad (1.8)$$

The authors examined several mathematical properties and proposed a further generalization based on the Jensen information measure, termed the Jensen FCRI. These developments offer powerful tools for quantifying information divergence in reliability and survival analysis, particularly under model uncertainty. Recently, Shaha and Kayal (2025) studied the fractional cumulative past inaccuracy (FCPI) by replacing the SFs in (1.6) with the CDF and the logarithm with the inverse of the Mittag-Leffler function (see Mittag-Leffler 1903; Jumarie 2012). They investigated several properties and employed FCPI as an indicator for detecting chaotic behavior in chaotic maps and an application to survival analysis.

The FCRI is invariant under location shifts. That is, for any constant b , the FCRI remains unchanged when RVs X_1 and X_2 are shifted by b , meaning

$$\mathcal{K}_\beta(X_1, X_2) = \mathcal{K}_\beta(X_1 + b, X_2 + b).$$

The property of invariance is the fact that the FCRI depends solely on the survival functions (SFs) $S_X(w)$ and $S_Y(w)$, and not on the particular values the RVs assume. Specifically, as equation (1.4) shows, the integrand is a function of w only through the SFs, and hence the resulting measure is location invariant. While this property is mathematically pleasing, it might be restrictive in many actual applications, e.g., reliability engineering or computational neuroscience, where the actual magnitudes of the variables matter. To eliminate this limitation, Belis and Guiasu (1964) had proposed a weighted version of Shannon entropy based on the magnitude of the RV, thereby giving more weight to large values. Later, investigations on weighted entropy models in different frameworks have been carried out by many researchers, such as Misagh et al. (2011), Daneshi et al. (2019), Tahmasebi (2020) and Ben Hssain and Lakhnati (2024). Inspired by their approach, we extend this idea to define weighted version of FCRI which emphasizes the importance of larger values of RVs X and Y . Throughout the paper we have used non-negative absolutely continuous RVs.

The rest of paper is organized as follows: In section 2 we introduced the concept of WFCRI and establish some bounds and properties. In section 3, we propose the dynamical version of WFCRI. A non-parametric estimation is proposed in section 3. In section 4, we validate WFCRI using the Ricker and cubic maps and used proposed measure as an application of instability in time series data.

2 Weighted fraction cumulative residual inaccuracy measure

In this section, we define a new inaccuracy measure which is the weighted version of FCRI. For this we consider an increasing non-negative differentiable function such that $\Psi'(w) = \psi(w) \geq 0$.

Definition 2.1. *Let S_X and S_Y be SFs of the RVs X and Y , respectively. Then the weighted fractional cumulative residual inaccuracy (WFCRI) is defined as*

$$\mathcal{K}_\beta^{\psi(w)}(X, Y) = \int_0^{+\infty} \psi(w) S_X(w) (-\log(S_Y(w)))^\beta dw, \quad \beta > 0. \quad (2.1)$$

The inaccuracy measure defined in (2.1) indicates the error that the experimenter commits in estimating the probability of events occurring due to incorrect use of the G distribution rather than the correct distribution of F and also due to incorrect information in the observations. It is worthwhile to note that when $\beta = 1$, (2.1) becomes the WCRI given in (1.4) with coefficient $\frac{1}{\Gamma(\alpha+1)}$. Using the Maclourin series

$$-\log(1 - x) = \sum_{i=1}^n \frac{x^i}{i}.$$

Applying this in (2.1), we obtain

$$\mathcal{K}_\beta^{\psi(w)}(X, Y) = \int_0^{+\infty} \psi(w) S_X(w) \left(\sum_{i=1}^n \frac{F_Y^i(w)}{i} \right)^\beta dw, \quad \beta > 0.$$

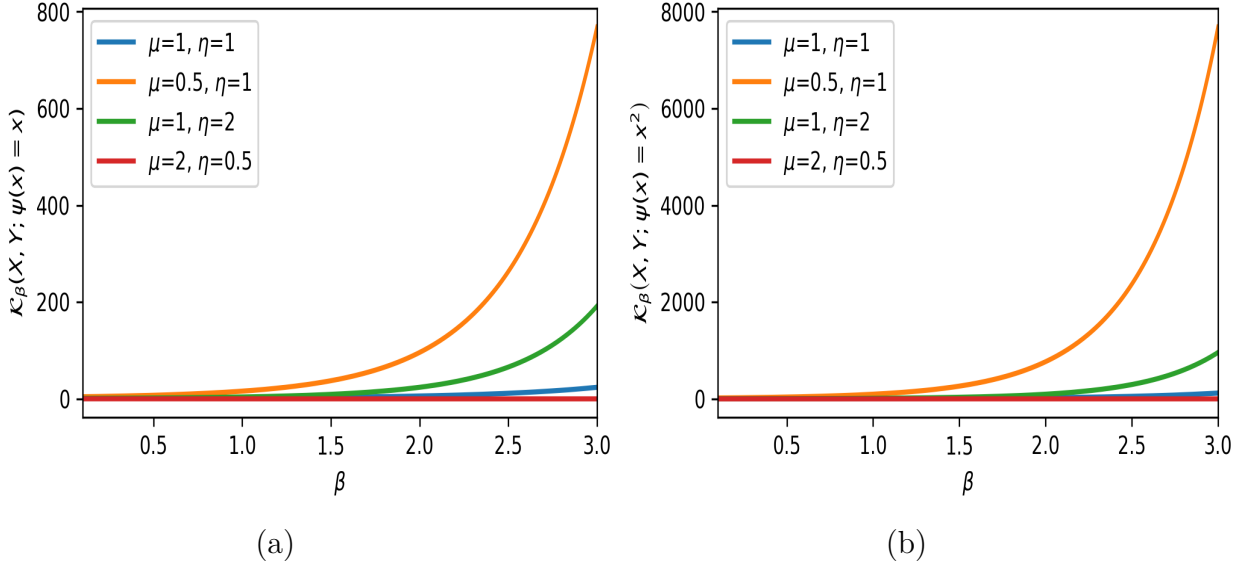


Figure 1: Plot of $\mathcal{K}_\beta^{\psi(w)}(X, Y)$ for Example 2.1 with $\psi(w) = w$ (left) and $\psi(w) = w^2$ (right).

now, we establish some bounds for the WFCRI. Now we illustrate the definition 2.1 with some well known distributions.

Example 2.1. Consider the SFs $S_X = e^{-\mu x}$ and $S_Y(w) = e^{-\eta w}$ for the RVs X and Y , respectively, and $x \geq 0, \mu, \eta > 0$. We have plotted the WFCRI for the weighted function $\psi(w) = w$ and $\psi(w) = w^2$ in Figure 1 (a) and (b), respectively.

Example 2.2. Consider the SFs $S_X(w) = (x+1)e^{-\mu x}$ and $S_Y(w) = e^{-\eta w^2}$ for the RVs X and Y , respectively, and $x \geq 0, \mu, \eta > 0$. We have plotted the WFCRI for the weighted function $\psi(w) = w$ and $\psi(w) = w^2$ in Figure 1 (a) and (b), respectively.

It is evident from the Figure 1, Figure 2 and Figure 3 that WFCRI provides more information than FCRI. Now, we establish some bounds for the WFCRI.

Theorem 2.1. For two RVs X and Y with SFs S_X and S_Y , respectively. If $\mathcal{K}_\beta^{\psi(w)}(X, Y)$ is finite, then

1. $\mathcal{K}_\beta^{\psi(w)}(X, Y) \geq \int_0^{+\infty} \psi(w) S_X(w) (1 - S_Y(w))^\beta dw$.
2. $\mathcal{K}_\beta^{\psi(w)}(X, Y) \geq \delta(\beta) e^{H(w)}$, where $\delta(\beta) = e^{\int_0^{+\infty} f(w) \log[\psi(w) S_X(w) - \log(S_Y(w))] dw}$.

Proof. First part of the proof follows from a well know-inequality $\log x \leq 1 - x, \forall x \leq 1$. For the second part. Applying log-sum inequality, we obtain

$$\int_0^{+\infty} f(w) \log \left(\frac{f(w)}{\psi(w) S_X(w) (-\log(S_Y(w)))^\beta} \right) dw \geq \log \left(\frac{1}{\int_0^{+\infty} \psi(w) S_X(w) (-\log(S_Y(w)))^\beta dw} \right).$$

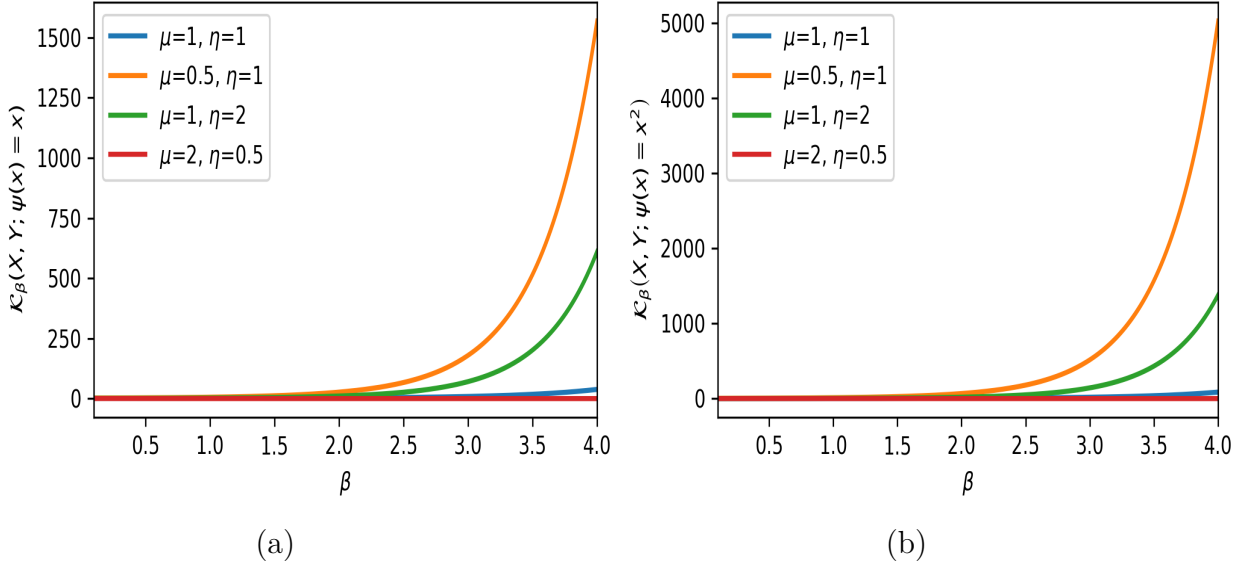


Figure 2: Plot of $\mathcal{K}_\beta^{\psi(w)}(X, Y)$ for Example 2.1 with $\psi(w) = w$ (left) and $\psi(w) = w^2$ (right).

Equivalently,

$$\log \left(\int_0^{+\infty} \psi(w) S_X(w) (-\log(S_Y(w)))^\beta dw \right) \geq \int_0^{+\infty} f(w) \log [\psi(w) S_X(w) - \log(S_Y(w))] dw - H(w).$$

□

Theorem 2.2. Let X, Y be RVs with SFs $S_X(\cdot)$ and $S_Y(\cdot)$, respectively. For $\beta > 0$,

1. If $X \leq_{st} Y$, then $\mathcal{K}_\beta^{\psi(w)}(Z, X) \leq \min \{H_\beta(X), H_\beta(Y)\}$.
2. If $X \geq_{st} Y$, then $\mathcal{K}_\beta^{\psi(w)}(Z, X) \geq \max \{H_\beta(X), H_\beta(Y)\}$.

Proof. If $X \leq_{st} Y$, then $S_X(w) \leq S_Y(w)$ for all x . Thus,

$$\begin{aligned} \mathcal{K}_\beta^{\psi(w)}(X, Y) &= \int_t^{+\infty} \psi(w) S_X(w) (-\log S_Y(w))^\beta dw \\ &\leq \int_t^{+\infty} \psi(w) S_Y(w) (-\log S_Y(w))^\beta dw = H_\beta(Y; t). \end{aligned}$$

Also $S_X(w) \leq S_Y(w) \implies (-\log S_X(w))^\beta \geq (-\log S_Y(w))^\beta$. It follows that

$$\begin{aligned} \mathcal{K}_\beta^{\psi(w)}(X, Y) &= \int_t^{+\infty} \psi(w) S_X(w) (-\log S_Y(w))^\beta dw \\ &\leq \int_t^{+\infty} \psi(w) S_Y(w) (-\log S_X(w))^\beta dw = H_\beta(X; t). \end{aligned}$$

Comparing both the inequality, we arrived at the desired result. Similarly, the second part of the proof. This completes the proof. □

Theorem 2.3. Let X, Y and Z be three RVs with SFs S, S_Y and H , respectively. Then

1. $\mathcal{K}_\beta^{\psi(w)}(Z, X) \geq \mathcal{K}_\beta^{\psi(w)}(Z, Y)$ if $X \leq_{st} Y$.
2. $\mathcal{K}_\beta^{\psi(w)}(X, Y) \geq \mathcal{K}_\beta^{\psi(w)}(X, Z)$ if $Y \leq_{st} Z$.

Proof. If $X \leq_{st} Y$, then $S_X(w) \leq S_Y(w)$ for all x . Equivalently,

$$\psi(w)S_Z(w) (-\log S_X(w))^\beta \geq \psi(w)S_Z(w) (-\log S_Y(w))^\beta.$$

Now, multiplying both sides by $\psi(w)$ and integrating both sides we obtain the desired result. \square

Theorem 2.4. Let X, Y and Z are RVs with SFs S, S_Y and \bar{H} , respectively. If $X_{st} \leq Y \leq_{st} Z$, then

$$\mathcal{K}_\beta^{\psi(w)}(X, Y) + \mathcal{K}_\beta^{\psi(w)}(Y, Z) \leq 2\mathcal{K}_\beta^{\psi(w)}(X, Z).$$

Proof. The proof directly follows from the definition of the WFCRI measure. \square

Theorem 2.5. Suppose X_1, X_2, Y_1 and Y_2 are RVs with $Y_1 = aX_1 + b$ and $Y_2 = aX_2 + b, a > 0, b \geq 0$. Then, for $\beta > 0$, we have

$$\mathcal{K}_\beta^{\psi(w)}(Y_1, Y_2) = \alpha \mathcal{K}_\beta^{\psi(ax+b)}(X_1, X_2).$$

Proof. The SFs of Y_1 and Y_2 are $S_{Y_1}(w) = S_{X_1}\left(\frac{w-b}{a}\right)$ and $S_{Y_2}(w) = S_{X_2}\left(\frac{w-b}{a}\right)$, respectively. Now, from the definition of WFCRI measure in (2.1), we have

$$\begin{aligned} \mathcal{K}_\beta^{\psi(w)}(Y_1, Y_2) &= \int_0^{+\infty} \psi(w)S_{Y_1}(w) (-\log S_{Y_2}(w))^\beta dw \\ &= \int_b^{+\infty} \psi(w) S_{X_1}\left(\frac{w-b}{a}\right) \left(-\log S_{X_2}\left(\frac{w-b}{a}\right)\right)^\beta dw \\ &= a \int_0^{+\infty} \psi(aw+b)S_{X_1}(w) (-\log S_{X_2}(w))^\beta dw \end{aligned}$$

Thus, the proof is completed. \square

Theorem 2.6. Let X be a RV with SF S_X . Then, for $\gamma \in (0, 1]$, we have

1. If X is IFRA and Y is DFRA, then $\frac{\mathcal{K}_\beta(X, Y; \psi(w)=x)}{\gamma} \geq \mathcal{K}_\beta^{\psi(w)}(S^\gamma, S_Y^\gamma)$.
2. If X is DFRA and Y is IFRA, then $\frac{\mathcal{K}_\beta^{\psi(w)}(X, Y)}{\gamma} \leq \mathcal{K}_\beta^{\psi(w)}(S^\gamma, S_Y^\gamma)$.

Proof. From the definition of IFRA and DFRA, for $\gamma \in (0, 1]$, $x > 0$, we have $S(\gamma x) \geq S^\gamma(w)$ and $S(\gamma x) \leq \overline{G}^\gamma(w)$. Thus

$$S(\gamma x) (-\log S_Y(\gamma x))^\beta \geq S^\beta(w) (-\log S_Y^\gamma(w))^\beta$$

Multiplying both sides by $\psi(w)$ and on integrating, we obtain

$$\frac{1}{\gamma} \int_0^{+\infty} \psi(w) S_X(w) (-\log S_Y(w))^\beta dw \geq \int_0^{+\infty} \psi(w) S^\beta(w) (-\log S_Y^\gamma(w))^\beta dw.$$

A similar analogy follows for the second part of the theorem. This concludes the proof. \square

Theorem 2.7. *If X and Y be non-negative RVs with SFs S and S_Y , respectively. Then*

$$\Gamma(\alpha + 1) CRE_\beta^{\psi(w)}(w) \geq (\leq) \mathcal{K}_\beta^{\psi(w)}(X, Y).$$

Proof. If we assume that $S_X(w) \leq (\geq) S_Y(w)$, then

$$(-\log S_X(w))^\beta \geq (\leq) (-\log S_Y(w))^\beta. \quad (2.2)$$

The above inequality holds since $f(z) = z^q$ is increasing for $z \geq 0$ and $q > 0$. Multiplying both sides by $\psi(w)$ and on integrating, we obtain

$$\int_0^{+\infty} \psi(w) S_X(w) (-\log S_X(w))^\beta dw \geq (\leq) \int_0^{+\infty} \psi(w) S_X(w) (-\log S_Y(w))^\beta dw.$$

This completes the proof. \square

Theorem 2.8. *Let X and Y be non-negative RVs with SFs S and S_Y , respectively and $\psi(w) = (\zeta)^\beta$, $\zeta(w) \geq 0$, we have*

$$\mathcal{K}_\beta^{\psi(w)}(X, Y) \geq (\leq) (FCRI_w(S, S_Y; \zeta(w)))^\beta \text{ for } \beta > 1 (0 < \beta < 1).$$

Proof. Let $\beta \geq 1$. Then for $x > 0$, $S_X(w) \geq (S_X(w))^\beta$. From (2.1), we have

$$\begin{aligned} \mathcal{K}_\beta^{\psi(w)}(X, Y) &= \int_0^{+\infty} \psi(w) S_X(w) (-\log(S_Y(w)))^\beta dw \\ &\geq \int_0^{+\infty} \psi(w) S^\beta(w) (-\log S_Y(w))^\beta dw \\ &= \int_0^{+\infty} (\zeta(w) S(w) (-\log S_Y(w)))^\beta dw. \end{aligned}$$

Let $\Delta(w) = \zeta(w) S_X(w) (-\log S_Y(w))^\beta$ and $g(\Delta(w)) = (\zeta(w) S_X(w) (-\log S_Y(w))^\beta)^\beta$. Since $g(z) = z^\beta$ is convex in $z \geq 0$, for $\beta \geq 1$. Using Jensen's inequality, we obtain the desired result. This completes the proof. \square

Consider a mixture hazards model of two hazard rate functions r_1 and r_2 as follows

$$r_p(w) = pr_1(w) + (1-p)r_2(w), \quad p \in (0, 1), \quad x > 0. \quad (2.3)$$

The SF corresponding to the mixture hazards model in (2.3) is given by

$$r_p(w) = pr_1(w) + (1-p)r_2(w), \quad p \in (0, 1), \quad x > 0. \quad (2.4)$$

The WFCRI measure is then obtained from (2.4) as follows.

Theorem 2.9. *An upper bound for the WFCRI measure of model in (14) is given by*

$$\mathcal{K}_\beta^{\psi(w)}(S_p, S_Y) \leq p\mathcal{K}_\beta^{\psi(w)}(S_1, S_Y) + (1-p)\mathcal{K}_\beta^{\psi(w)}(S_2, S_Y).$$

Proof. From the definition of the WFCRI measure and making use of arithmetic mean-geometric mean inequality, we have

$$\begin{aligned} \mathcal{K}_q(S_p, S_Y) &= \int_0^{+\infty} \psi(w) S_1^p(w) S_2^{1-p}(w) (-\log S_Y(w))^q dw \\ &\leq \int_0^{+\infty} \psi(w) (pS_1(w) + (1-p)S_2(w)) (-\log S_Y(w))^q dw. \end{aligned}$$

This completes the proof. □

3 Dynamic Fractional Cumulative Residual Entropy

In this section, we introduce a dynamical formulation of the WFCRI by drawing inspiration from the reliability theory. Consider a system that begins operation at time 0 and is found to have failed at a predetermined inspection time $t \in (0, s)$. Here, the focus of uncertainty shifts to the past, as the exact time of system failure is unknown but known to have occurred within the interval $(0, t)$, that is, before the inspection took place. Di Crescenzo et al. (2021) studied the fractional generalized cumulative entropy for the dynamical system. Let X denote the RV representing the time of the system failure. Shaha and Kayal (2025) studied the FCPI for the dynamical system. Motivated by these studies, we introduce the dynamical version of WFCRI, which is known as dynamical weighted fractional cumulative residual inaccuracy (DWFCRI). Let S_X and S_Y be SFs of the RVs X and Y , respectively. Then, the DWFCRI measure is defined as

$$\mathcal{K}_\beta^{\psi(w)}(X, Y; t) = \int_t^{+\infty} \psi(w) \frac{S_X(w)}{S_X(t)} \left(-\ln \frac{S_Y(w)}{S_Y(t)} \right)^\beta dw, \quad \beta > 0, t > 0. \quad (3.1)$$

When $t = 0$ DWFCRI coincide with the WFCRI. It is not hard to see that when β tends to 1, then WFCRI coincide with the weighted cumulative inaccuracy measure (Daneshi et al., 2019).

Similar to the Theorem 2.4, we get the following result concerning the effect of an affine transformation. For the brevity the proof is omitted.

Theorem 3.1. Suppose X_1, X_2, Y_1 and Y_2 are RVs with $Y_1 = aX_1 + b$ and $Y_2 = aX_2 + b, a > 0, b \geq 0$. Then, for $\beta > 0$, we have

$$\mathcal{K}_\beta^{\psi(w)}(Y_1, Y_2; t) = \alpha \mathcal{K}_\beta^{\psi(aw+b)}\left(X_1, X_2; \frac{t-b}{a}\right).$$

Theorem 3.2. For two RVs X and Y with SFs S_X and S_Y , respectively. If $\mathcal{K}_\beta^{\psi(w)}(X, Y)$ is finite, then

1. $\mathcal{K}_\beta^{\psi(w)}(X, Y; t) \geq \int_t^{+\infty} \psi(w) \frac{S_X(w)}{S_X(t)} \left(1 - \frac{S_Y(w)}{S_Y(t)}\right)^\beta dw$.
2. $\mathcal{K}_\beta^{\psi(w)}(X, Y; t) \geq \delta(\beta) e^{H(X; t)}$, where $\delta(\beta) = e^{\int_0^{+\infty} f(w) \log[\psi(w) S_X(w) - \log(S_Y(w))] dw}$.

Theorem 3.3. Let $S_X(\cdot)$ and $S_Y(\cdot)$ are SFs of X and Y , respectively. For $\beta > 0, t > 0$

1. If $X \geq_{hr} Y$, then $\mathcal{K}_\beta^{\psi(w)}(X, Y; t) \geq \max\{H^{\psi(w)}(X), H_\alpha(Y; t)\}$.
2. If $X \leq_{hr} Y$, then $\mathcal{K}_\beta^{\psi(w)}(X, Y; t) \leq \min\{H^{\psi(w)}(X), H_\alpha(Y; t)\}$.

Proof. If $X \geq_{hr} Y$, then $\frac{S_X(x)}{S_X(t)} \geq \frac{S_Y(x)}{S_Y(t)}$. From (3.1),

$$\begin{aligned} \mathcal{K}_\beta^{\psi(w)}(X, Y; t) &= \int_t^{+\infty} \psi(w) \frac{S_X(w)}{S_X(t)} \left(-\ln \frac{S_Y(w)}{S_Y(t)}\right)^\beta dw \\ &\geq \int_t^{+\infty} \psi(w) \frac{S_Y(w)}{S_Y(t)} \left(-\ln \frac{S_Y(w)}{S_Y(t)}\right)^\beta dw. \end{aligned}$$

Now, $\frac{S_X(x)}{S_X(t)} \geq \frac{S_Y(x)}{S_Y(t)}$ implies $\left(-\log \frac{S_X(x)}{S_X(t)}\right)^\beta \leq \left(-\log \frac{S_Y(x)}{S_Y(t)}\right)^\beta$. From both the inequality, we obtain $\mathcal{K}_\beta^{\psi(w)}(X, Y; t) \geq \max\{H^{\psi(w)}(X), H_\alpha(Y; t)\}$. \square

3.1 DWFCRI under Proportional hazard model

The hazard rate (HR) function of a continuous RV X , denoted by $r_X(x)$, is defined as $r_X(x) = \frac{f_X(x)}{S_X(x)}$, where $f_X(x)$ is the pdf of X , and $S_X(x)$ is its SF. Intuitively, the hazard rate describes the instantaneous rate of failure at time x , given that the event has not occurred before time x . Now, consider two RVs X and Y with hazard functions $r_X(x)$ and $r_Y(x)$, respectively. The RVs X and Y are said to satisfy the Proportional Hazards Model (PHM) if there exists a positive constant $\alpha > 0$ such that $r_Y(x) = \alpha r_X(x)$, or equivalently, the SFs satisfy: $S_Y(x) = (S_X(x))^\alpha$. This model was introduced in a seminal paper by Cox (1972), and later extended and discussed by researchers such as Efron (1981). The PHM is widely used in survival analysis, particularly in medical statistics and reliability engineering, where it captures the effect of covariates (such as treatment, environment, or subject characteristics) on the lifetime of an individual or system. The DFRCRI measure of the PHR models of U and V with respective SFs $(\bar{S}_U(\cdot))^\alpha$ and $(\bar{S}_V(\cdot))^\alpha$, is defined as

$$\mathcal{K}_\beta^{\psi(w)}(U, V; t) = \int_t^{+\infty} \psi(w) \left(\frac{S_X(w)}{S_X(t)}\right)^\alpha \left(-\log \left(\frac{S_X(w)}{S_X(t)}\right)^\alpha\right)^\beta dw. \quad (3.2)$$

Theorem 3.4. Let $S_X(\cdot)$ and $S_Y(\cdot)$ are SFs of the RVs X and Y , respectively. For two PHR RVs U and V , we obtain

$$K_\beta^{\psi(w)}(U, V; t) = \frac{\alpha^\beta}{S_X^{\alpha-1}(t)} \mathcal{K}_\beta^{\psi(w)}(X, Y; t), \quad \beta, t > 0.$$

Proof. From (3.2), we have

$$\begin{aligned} K_\beta^{\psi(w)}(U, V; t) &= \int_t^{+\infty} \psi(w) \left(\frac{S_X(w)}{S_X(t)} \right)^\alpha \left(-\log \left(\frac{S_Y(w)}{S_Y(t)} \right) \right)^\beta dw \\ &= \alpha^\beta \int_t^{+\infty} \psi(w) \left(\frac{S_X(w)}{S_X(t)} \right)^\alpha \left(-\log \frac{S_Y(w)}{S_Y(t)} \right)^\beta dw \\ &\leq \frac{\alpha^\beta}{S_X^{\alpha-1}(t)} \int_t^{+\infty} \psi(w) \frac{S_X(w)}{S_X(t)} \left(-\log \frac{S_Y(w)}{S_Y(t)} \right)^\beta dw \\ &= \frac{\alpha^\beta}{S_X^{\alpha-1}(t)} \mathcal{K}_\beta^{\psi(w)}(X, Y; t). \end{aligned}$$

This concludes the proof. \square

Theorem 3.5. Let X, Y, U and V be the RVs with SFs $S_X(\cdot), S_Y(\cdot), (S_X(\cdot))^\alpha$ and $(S_Y(\cdot))^\alpha$, respectively. If $X \leq_{hr} Y$, then

$$K_\beta^{\psi(w)}(U, V; t) \leq \frac{\alpha^\beta}{S_X^{\alpha-1}(t)} \min\{H_\beta(X; t), H_\beta(Y; t)\}.$$

Proof. If $X \leq_{hr} Y$, then $\frac{S_X(x)}{S_X(t)} \leq \frac{S_Y(x)}{S_Y(t)}$. Thus, from (3.2), we obtain

$$\begin{aligned} K_\beta^{\psi(w)}(U, V; t) &\leq \frac{\alpha^\beta}{S_X^{\alpha-1}(t)} \int_t^{+\infty} \psi(w) \frac{S_X(w)}{S_X(t)} \left(-\log \frac{S_Y(w)}{S_Y(t)} \right)^\beta dw \\ &\leq \frac{\alpha^\beta}{S_X^{\alpha-1}(t)} \int_t^{+\infty} \psi(w) \frac{S_X(w)}{S_X(t)} \left(-\log \frac{S_X(w)}{S_X(t)} \right)^\beta dw \\ &= \frac{\alpha^\beta}{S_X^{\alpha-1}(t)} H_\beta(X; t) \end{aligned} \tag{3.3}$$

and

$$\begin{aligned} K_\beta^{\psi(w)}(U, V; t) &\leq \frac{\alpha^\beta}{S_X^{\alpha-1}(t)} \int_t^{+\infty} \psi(w) \frac{S_X(w)}{S_X(t)} \left(-\log \frac{S_Y(w)}{S_Y(t)} \right)^\beta dw \\ &\leq \frac{\alpha^\beta}{S_X^{\alpha-1}(t)} \int_t^{+\infty} \psi(w) \frac{S_Y(w)}{S_Y(t)} \left(-\log \frac{S_Y(w)}{S_Y(t)} \right)^\beta dw \\ &= \frac{\alpha^\beta}{S_X^{\alpha-1}(t)} H_\beta(Y; t). \end{aligned} \tag{3.4}$$

Combining the equations (3.3) and (3.4) gives the desired result. \square

4 Non-parametric estimation

In the next section, we empirically estimate the WFCRI under PHR model. Suppose a random sample (X_1, \dots, X_n) is drawn from a population with SF $F_X(\cdot)$. The order statistics corresponding to the random sample (X_1, \dots, X_n) are denoted as $X_{1:n} \leq \dots \leq X_{n:n}$, where $X_{1:n} = \min(X_1, \dots, X_n)$ and $X_{n:n} = \max(X_1, \dots, X_n)$. The empirical SF of $F_X(\cdot)$ is The empirical SF is

$$\widehat{S}_n(w) = \begin{cases} 0, & \text{if } w > X_{1:n}; \\ \frac{j}{n}, & \text{if } X_{j:n} \geq w > X_{j+1:n}; \\ 1, & \text{if } w \leq X_{n:n}. \end{cases} \quad (6.1)$$

where $j = 1, \dots, n-1$. For the RVs X and Y with corresponding SFs $S_X(\cdot)$ and $[S_X(\cdot)]^\alpha, \alpha > 0$, the WFCRI measure for weighted function $\psi(w) = w$ by using (6.1) is expressed as

$$\begin{aligned} \widehat{K}_\beta(\widehat{S}_n, \widehat{S}_n^\alpha; w) &= \int_0^{+\infty} w \widehat{S}_n(w) \left(-\log(\widehat{S}_n(w))^\alpha\right)^\beta dw \\ &= \gamma^\beta \sum_{j=1}^{n-1} \int_{X_{j:n}}^{X_{j+1:n}} w \widehat{S}_n(w) [-\log \widehat{S}_n(w)]^\beta dw \\ &= \gamma^\beta \sum_{j=1}^{n-1} \frac{(X_{j+1:n})^2 - (X_{j:n})^2}{2} \left(1 - \frac{j}{n}\right) \left(-\log\left(1 - \frac{j}{n}\right)\right)^\beta. \end{aligned} \quad (4.1)$$

It is worth noting that $K_\beta(\widehat{S}_n, \widehat{S}_n^\alpha; x)$ is indeed the WFCRE given in (\star) with coefficient α^γ and $\psi(w) = w$.

The following theorem states that this estimator converges almost surely (a.s.) to $\mathcal{K}_\beta^{\psi(w)}(X, Y)$.

Theorem 4.1. *Let $X \in L^m$, for $m > 2$. Then, $\widehat{K}_\beta^{\psi(w)}(\widehat{S}_n, \widehat{S}_n^\alpha) \rightarrow \mathcal{K}_\beta^{\psi(w)}(S, S^\alpha)$ a.s.*

Proof. We have

$$\begin{aligned} \mathcal{K}_\beta^{\psi(w)}(X, Y) &= \gamma^\beta \left(\int_0^1 w \widehat{S}_n(w) \left(-\log(\widehat{S}_n(w))\right)^\beta dw + \int_1^\infty w \widehat{S}_n(w) \left(-\log(\widehat{S}_n(w))\right)^\beta dw \right) \\ &= \gamma^\beta (A_1 + A_2). \end{aligned}$$

Using Glivenko-Centelli theorem and dominated convergence theorem, we have

$$\lim_{n \rightarrow \infty} A_1 = \int_0^1 w S(w) \left(-\log(S(w))\right)^\beta dw$$

□

4.1 Simulation Study

In this section, we assess the performance of the estimator defined in Equation (3.1). Data are generated from an exponential distribution with rate parameter $\lambda = 2$. Using Monte

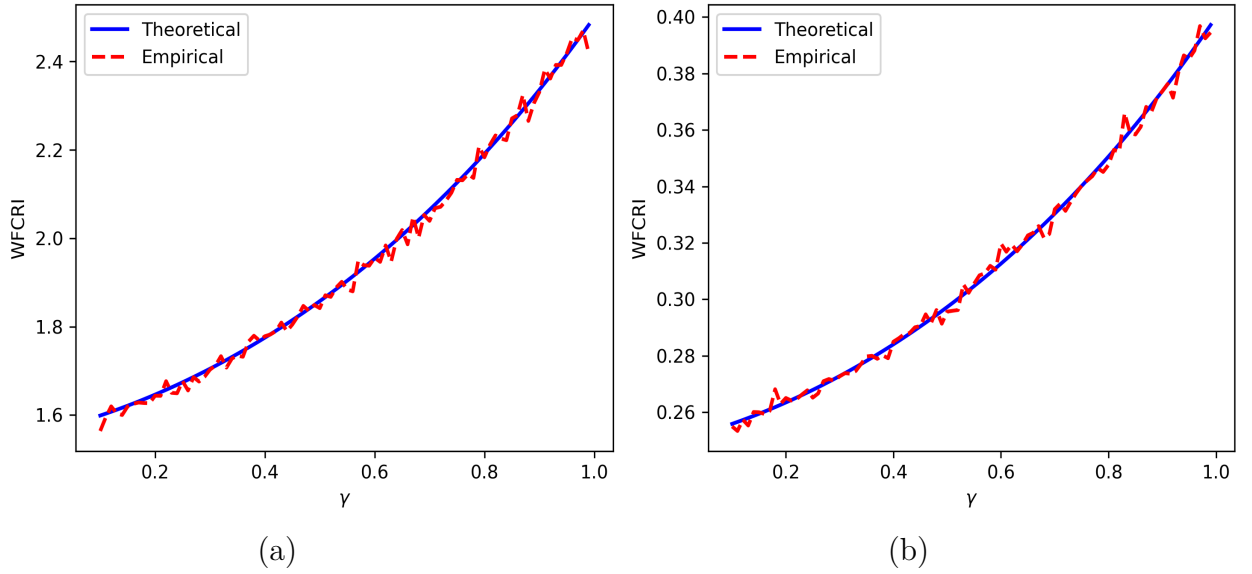


Figure 3: Plot of theoretical and empirical value of WFCRI for exponential distribution with parameter $\lambda = 0.8$ (left) and $\lambda = 2$ (right).

Carlo simulations, we examine the behavior of the estimator across varying sample sizes: $n = 50, 100, 150,$ and 200 . Each simulation is repeated 10,000 times. The results, including absolute bias and mean squared error (MSE), are summarized in Table 1, where MSE values are presented in parentheses. To study the effect of the tuning parameter γ , we evaluate the estimator for $\gamma = 0.5$ and range of values: $\beta = 0.2, 0.4, 0.6, 0.8,$ and 1 . This analysis allows us to investigate the robustness and performance of the estimator under varying degrees of influence controlled by γ . The results demonstrate that the estimator performs consistently across all tested γ values, with decreasing MSE as the sample size increases, further highlighting the estimator's consistency. This outcome aligns with theoretical expectations and affirms the reliability of the proposed estimator, particularly under larger sample sizes and different values of γ . To further validate these findings, we compare theoretical and empirical estimates for $\lambda = 0.8$ and $\lambda = 2$, illustrated in Figures 1 and 2, respectively. These plots are based on a large sample size ($n = 10,000$) and are averaged over 10 simulation runs. The close agreement between the theoretical and empirical curves in both figures reinforces the estimator's accuracy and consistency across different scenarios and parameter values.

5 Applications

In this section, we present two applications of the WFCRI under the PHR model. First, we demonstrate that WFCRI can effectively detect chaotic behavior in deterministic dynamical systems. Second, we apply this measure to financial data to quantify uncertainty in stock price movements.

Table 1: Absolute bias and MSE of $\widehat{\mathcal{K}}_{\beta}^{\psi(w)=w}(\widehat{F}_n, \widehat{F}_n^{\alpha})$ for different values of γ .

$\beta \backslash n$	50	100	150	200
0.2	-0.00438507 (0.006166726 9)	-0.002202962 (0.003171737)	-0.001530227 (0.002109278)	-0.00133209 (0.001598269)
0.4	-0.008335939 (0.006594374)	-0.005061422 (0.003420775)	-0.003307744 (0.00232513)	-0.002782336 (0.001745512)
0.6	-0.01389529 (0.007253)	-0.0082854 (0.003817273)	-0.005752369 (0.002633498)	-0.004548167 (0.002005892)
0.8	-0.01993732 (0.008188544)	-0.01199614 (0.004483481)	-0.008703718 (0.003136844)	-0.007123592 (0.00240045)
1.2	-0.03621987 (0.01181693)	-0.02270142 (0.00682418)	-0.01738631 (0.00489378)	-0.0139283 (0.003819348)
2.2	-0.1357006 (0.0455673)	-0.09405404 (0.02980198)	-0.07502776 (0.02259248)	-0.06389411 (0.01841551)

5.1 Application to Chaotic Maps

We begin by empirically estimating the WFCRI under the PHR model for chaotic maps. Chaos theory is instrumental in describing complex systems that exhibit high sensitivity to initial conditions and seemingly random behavior. In such cases, traditional statistical or computational models may fall short. The WFCRI, by incorporating both distributional and temporal characteristics, serves as a robust measure for identifying the underlying uncertainty in chaotic time series. In this study, we consider two chaotic maps: the Ricker map and the cubic map.

5.1.1 Ricker Map

The Ricker map (Ricker, 1954) is defined as $x_{n+1} = x_n e^{r(1-x_n)}$, where $r > 0$ is a growth rate parameter. This map models population dynamics with density-dependent regulation and has two fixed points: $x = 0$ and $x = 1$. The fixed point at $x = 0$ is always unstable for $r > 0$, while the fixed point at $x = 1$ is locally stable when $0 < r < 2$. As r increases beyond 2, the system undergoes a period-doubling cascade, eventually leading to chaotic behavior. To generate simulated data with a sample size of $n = 10,000$, we use an initial value $x_0 = 0.01$ and let $r \in [1, 5]$. The bifurcation diagram (see Figure 4(a)) of the Ricker map illustrates the transition from stable fixed points to periodic cycles and ultimately to chaos, depending on the value of r . For example, the system converges to a stable fixed point at $r = 1$, while it exhibits chaotic behavior at $r = 3$, $r = 4$, and $r = 5$. The graphical presentation of the empirical WFCRI measure in Equation (6.2) is shown in Figure 4(a) for various values of β and selected values of $r = 2, 3.5, 4, 4.5$, and 5. Additionally, we plot the WFCRI measure for $\beta \in [1, 4]$ and $r \in [2, 4]$. From Figures 4(a) and 5(a), it is evident that the WFCRI measure increases for $r > 2.5$, corresponding to the onset of chaotic dynamics, as expected.

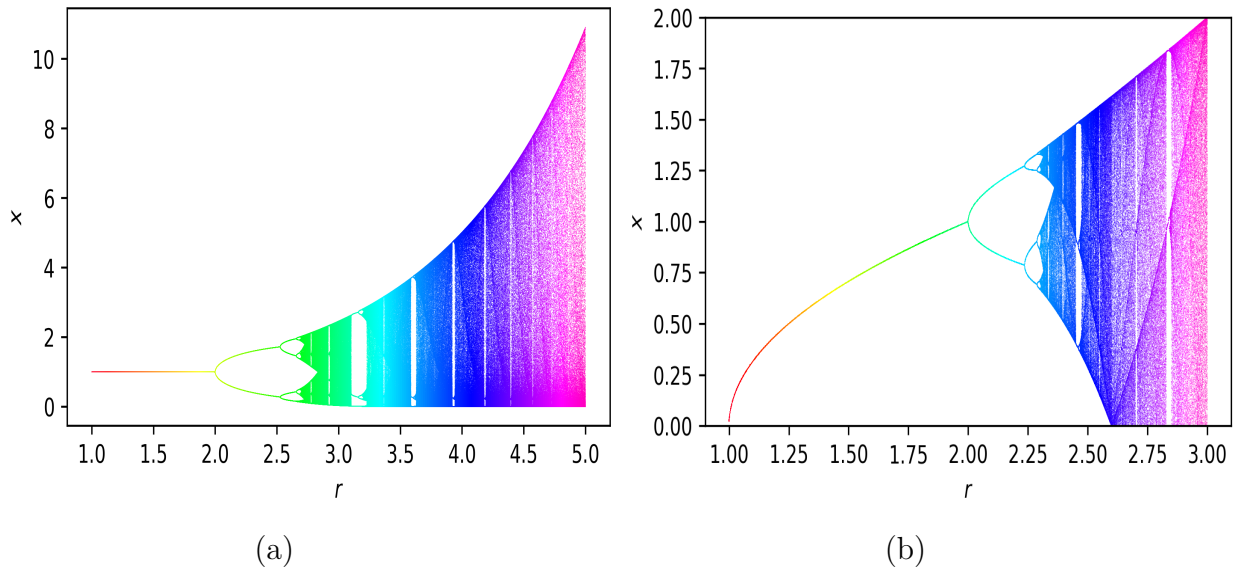


Figure 4: Bifurcation diagram of Ricker map (left) and cubic map (right).

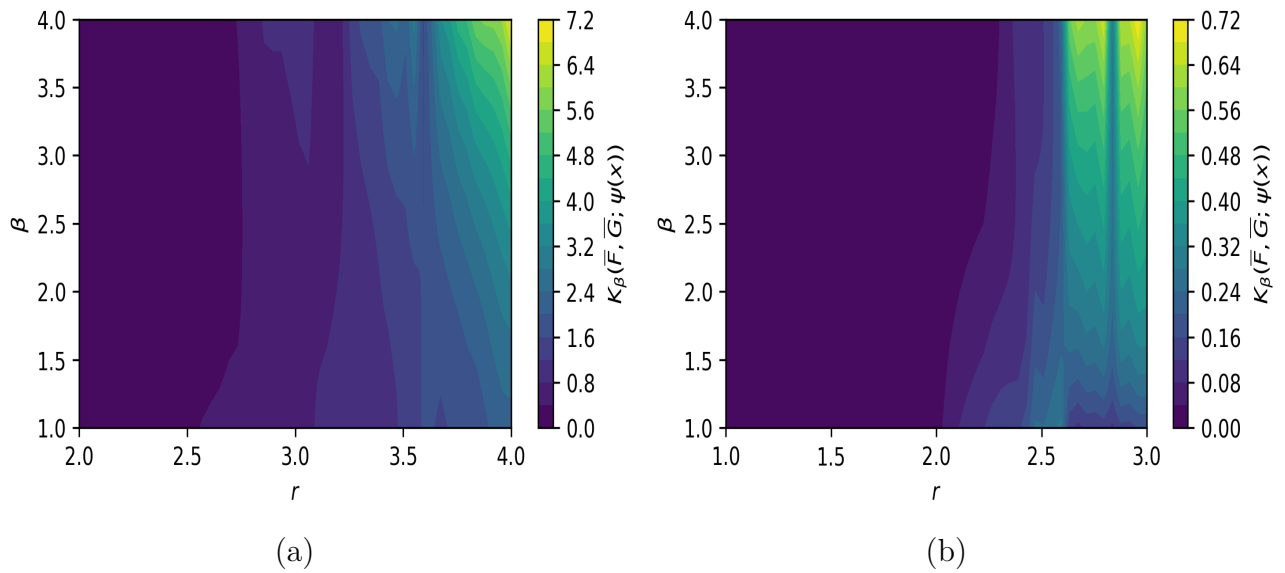


Figure 5: Plot of $K_\beta(\widehat{F}_n, \widehat{F}_n^\alpha; \psi(w) = w)$ for Ricker map (left) and Cubic map (right) for $r \in [2, 4]$ and $\beta \in [1, 4]$.

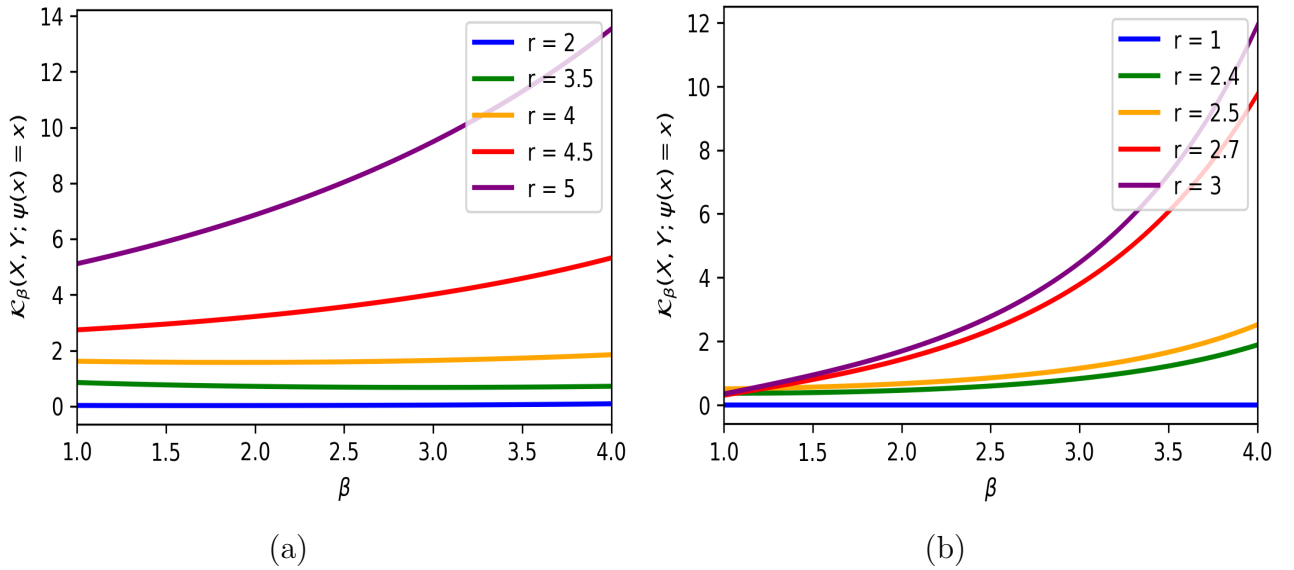


Figure 6: Plot of $K_\beta(\widehat{F}_n, \widehat{F}_n^\alpha; \psi(w) = w)$ for Ricker map (left) and Cubic map (right) for different values of r with $\beta \in (1, 4)$.

5.1.2 Cubic Map

The cubic map (Malik et al., 2020) is defined as $x_{n+1} = rx_n - x_n^3$, where r is a control parameter. This simple nonlinear system exhibits a variety of dynamical behaviors—including fixed points, periodic orbits, and chaos—depending on the value of r . The dynamics arise from the interplay between linear growth and nonlinear damping. To generate simulated data of size $n = 10,000$, we use an initial condition $x_0 = 0.01$ and vary r in the interval $[1, 3]$. The bifurcation diagram shown in Figure 4(b) illustrates how the system transitions from stable fixed points to periodic orbits and eventually to chaotic dynamics. Notably, the degree of chaos becomes pronounced as r approaches higher values, with maximum chaotic behavior observed near $r = 3$. We compute the WFCRI measure for the cubic map to quantify this dynamical complexity. Specifically, we plot WFCRI for $r = 1, 2.4, 2.5, 2.7$, and 3 , with $\beta \in (1, 4)$. As shown in Figure 6(b), the WFCRI value is close to zero at $r = 1$, indicating low uncertainty, while it increases significantly for $r > 2$, reflecting the onset of chaos. Additionally, a surface plot of WFCRI for $r \in [1, 3]$ and $\beta \in [1, 4]$ further demonstrates the measure’s effectiveness in detecting chaotic behavior in the cubic map. As r increases beyond 2, the WFCRI clearly captures the growing uncertainty and complexity of the system’s dynamics.

5.2 Detecting Market Uncertainty Using WFCRI

We apply the Weighted Fractional Cumulative Residual Information (WFCRI) under the Proportional Hazard Rate (PHR) model for $\gamma = 5$ and $\gamma = 10$ with $\beta \in (0, 2)$ to assess temporal uncertainty in the Indian stock market, using daily closing prices of the Nifty 50 index from January 1, 2000 to December 31, 2020. This dataset comprises approximately 5,200 daily

observations. Let P_t denote the closing price on day t ; the daily log returns are computed as

$$R_t = \log(P_t) - \log(P_{t-1}),$$

which are then shifted to non-negative values by defining $Z_t = R_t - \min_t R_t$, thereby satisfying the non-negativity requirement of WFCRI. To capture the evolving structure of uncertainty, we compute WFCRI over a rolling window of 250 trading days (roughly one year), with updates every 100 days. This yields a time series of WFCRI estimates that reflect the market's information uncertainty across different time horizons and fractional orders. Figure 1 presents the time series of R_t , where significant negative spikes mark episodes of acute market stress. Noteworthy among these are:

- **May 2004 (UPA 1 election crash):** The BSE plunged 15.52% in a single day—its largest percentage fall ever.
- **2006–2009 financial turmoil:** Including January 2008's "Black Monday," March 2008 declines, and the major crash of October 2008.
- **March 2020 (COVID-19 pandemic):** A sequence of historic losses culminating in a 3,900-point drop on March 23.

(For further historical context, see https://en.wikipedia.org/wiki/Stock_market_crashes_in_India.) Figure 2 displays a contour plot of the WFCRI values, with the horizontal axis representing the fractional order $\beta \in (0, 2)$, and the vertical axis denoting time. The color gradient reflects the magnitude of WFCRI, which quantifies the weighted residual uncertainty of the shifted return distribution Z_t . Compared to the traditional Fractional Cumulative Residual Entropy (FCREn), WFCRI incorporates a hazard-based weighting mechanism that enhances sensitivity to tail events and temporal irregularities. This makes WFCRI more effective in detecting structural breaks and crisis periods in financial time series, as evidenced by its sharper contrast and finer resolution in the contour plots. Hence, WFCRI provides a more nuanced and robust assessment of market uncertainty dynamics over time. We also plotted the FCREn defined in (1.9) for $\beta \in (0, 2)$ in Figure 9. The WFCRI surface reveals that for $\gamma = 5$ and $\gamma = 10$, the measure is highly sensitive to regime changes and captures crisis periods more distinctly. We also observe from Figure 9(a) and 9(b) that WFCRI measure provided more information than the FCREn for $\gamma = 5$ and $\gamma = 10$. In summary, the combination of the log return series and the fractional entropy surface provides a compelling picture of market uncertainty. The fractional nature of WFCRI enhances its ability to detect systemic events, outperforming FCRE.

6 Conclusion

In recent years, several inaccuracy measures have been studied, including Kerridge, Rényi, Tsallis inaccuracy, and their weighted variants. In this paper, we propose a new measure called the WFCRI. We establish several bounds for the WFCRI and investigate its behavior under

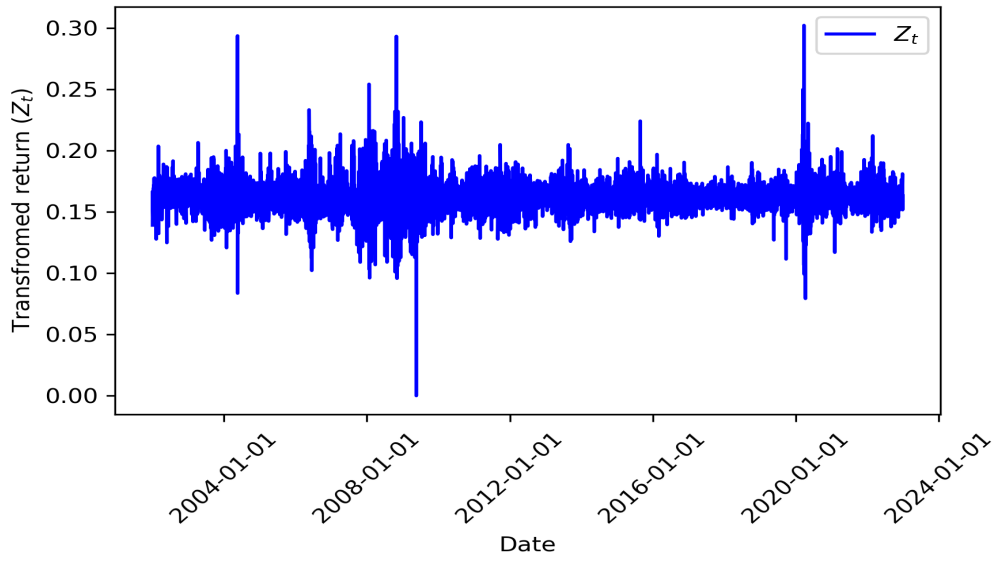


Figure 7: The contour plot illustrates the WFCRI under PHR model.

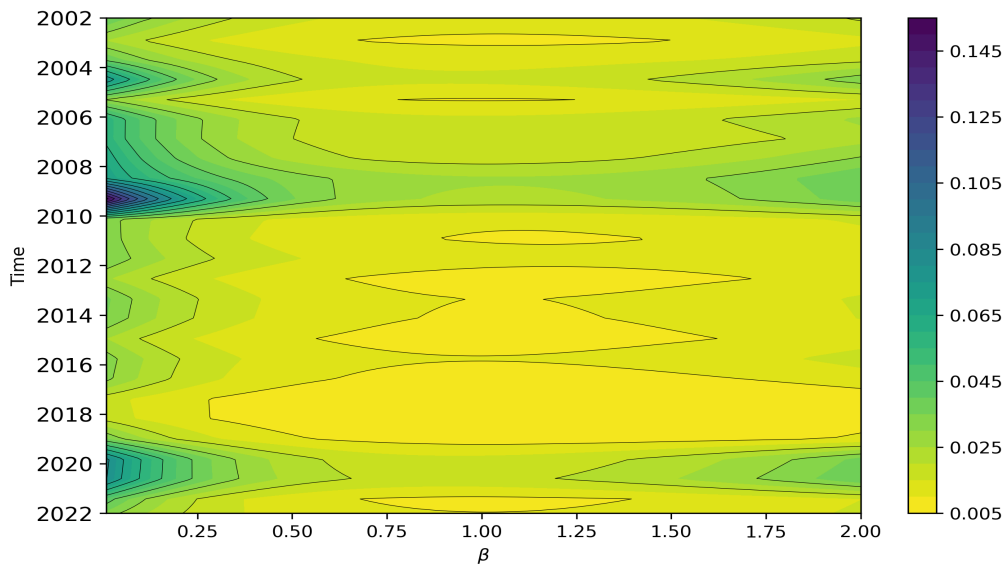


Figure 8: The contour plot illustrates the FCREn for $\beta \in (0, 2)$ (with a step size of 0.01) and time, where the vertical axis represents the center of each sliding window.

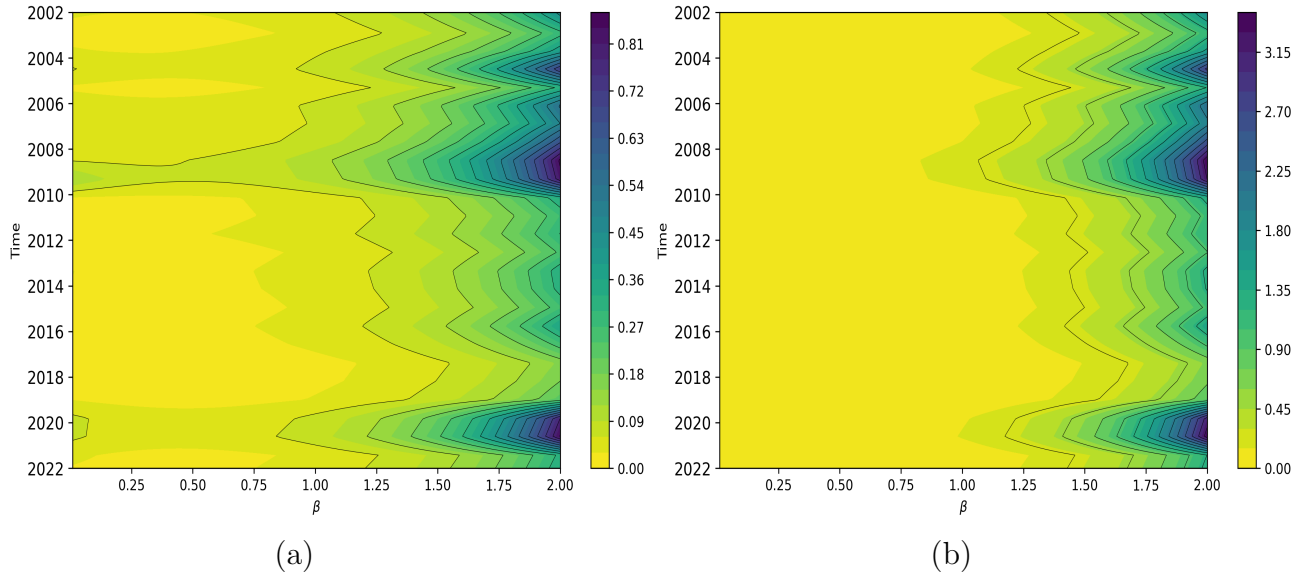


Figure 9: The contour plot illustrates the WFCRI under PHR model with $\gamma = 5$ (left) and $\gamma = 10$ (right) for $\beta \in (0, 2)$ (with a step size of 0.01) and time, where the vertical axis represents the center of each sliding window.

different stochastic orders. Furthermore, we demonstrate that WFCRI is a shift-dependent measure. We also examine the WFCRI under PHR model, and under a mixture of hazard models, where we establish additional bounds. A dynamical version of the WFCRI is introduced, along with theoretical bounds for this extension. To validate the applicability of our proposed measure, we present an empirical estimation procedure for the WFCRI and conduct simulations. The results show that the MSE decreases as the sample size increases, indicating consistency. Additionally, we analyze two chaotic maps: the Ricker map and the cubic map and demonstrate that the WFCRI effectively detects the chaotic nature of these systems. Finally, we apply the WFCRI to time series data to detect potential instabilities. Our results show that the WFCRI attains higher values during periods of crisis, thereby demonstrating its effectiveness in capturing structural changes and its practical relevance in real-world applications.

Data Availability

The Nifty 50 data is obtained from <https://www.kaggle.com/datasets/adarshde/nifty-50-data-1990-2024>.

Conflict of Interest

The authors declare there is no conflict of interest.

References

- [1] Shannon, C. E. (1948). A Mathematical Theory of Communication. The Bell System Technical Journal, 27(4), 623-656.
- [2] MacKay, D. (2003) Information Theory, Inference, and Learning Algorithms. Cambridge University Press, Cambridge.
- [3] Ubriaco MR. Entropies based on fractional calculus. Phys Lett A 2009;373(30):2516-19.
- [4] Daneshi, S., Nezakati, A. & Tahmasebi, S. On weighted cumulative past (residual) inaccuracy for record values. J Inequal Appl 2019, 134 (2019).
- [5] Rao M, Chen Y, Vemuri BC, Wang F (2004) Cumulative residual entropy: a new measure of information. IEEE Trans Inf Theory 50(6):1220–1228.
- [6] Nath P (1968) Inaccuracy and coding theory. Metrika 13(1):123–135.
- [7] Bhatia PK (1995) Useful inaccuracy of order and 1.1 coding. Soochow J Math 21(1):81–87.
- [8] Kundu C, Nanda AK (2015) Characterizations based on measure of inaccuracy for truncated RVs. Stat Pap 56(3):619–637.
- [9] Kundu C, Di Crescenzo A, Longobardi M (2016) On cumulative residual (past) inaccuracy for truncated RVs. Metrika 79(3):335–356.
- [10] Kayal S, Madhavan SS, Ganapathy R (2017) On dynamic generalized measures of inaccuracy. Statistica (Bologna) 77(2):133–148.
- [11] O. Kharazmi, J.E. Contreras-Reyes, N. Balakrishnan, Fisher-based inaccuracy information measure, Fluct. Noise Lett. (2024) 2550009.
- [12] O. Kharazmi, J.E. Contreras-Reyes, Belief inaccuracy information measures and their extensions, Fluct. Noise Lett. 23 (4) (2024) 2450041–2450199.
- [13] Xiong, H., Shang, P., and Zhang, Y. (2019). Fractional cumulative residual entropy. Communications in Nonlinear Science and Numerical Simulation, 78:104879.
- [14] Psarrakos G, Navarro J. Generalized cumulative residual entropy and record values. Metrika 2013;27:623–640.
- [15] Machado JT. Fractional order generalized information. Entropy 2014;16(4):2350–2361.
- [16] A. Di Crescenzo, S. Kayal, A. Meoli, Fractional generalized cumulative entropy and its dynamic version, Commun. Nonlinear Sci. Numer. Simul., 102 (2021), 105899.
- [17] Kumar V, Taneja HC (2015) Dynamic cumulative residual and past inaccuracy measures. J Stat Theory Appl 14:399–412.

- [18] O. Kharazmi, J.E. Contreras-Reyes, Fractional cumulative residual inaccuracy information measure and its extensions with application to chaotic maps, *Int. J. Bifurc. Chaos* 34 (01) (2024) 2450006.
- [19] Saha, S., Kayal, S.: Fractional cumulative past inaccuracy measure, its dynamic version and applications in survival analysis. *Physica D: Nonlinear Phenomena* 473, 134545 (2025).
- [20] G.M. Mittag-Leffler, Sur la nouvelle fonction $E_\alpha(x)$, *CR Acad. Sci. Paris* 137 (2) (1903) 554–558.
- [21] G. Jumarie, Derivation of an amplitude of information in the setting of a new family of fractional entropies, *Inform. Sci.* 216 (2012) 113–137.
- [22] Guiasu S (1971) Weighted entropy. *Rep Math Phys* 2(3):165–179.
- [23] Mirali, M., Baratpour, S., & Fakoor, V. (2016). On weighted cumulative residual entropy. *Communications in Statistics - Theory and Methods*, 46(6), 2857–2869.
- [24] Ricker, W. E. (1954) Stock and Recruitment *Journal of the Fisheries Research Board of Canada*, 11(5): 559–623.
- [25] Malik, D.S., Shah, T.: Color multiple image encryption scheme based on 3D-chaotic maps. *Math. Comput. Simulat.* 178, 646-666 (2020).
- [26] Daneshi, S., Nezakati, A. & Tahmasebi, S. On weighted cumulative past (residual) inaccuracy for record values. *J Inequal Appl* 2019, 134 (2019).
- [27] Misagh, F., Y. Panahi, G. H. Yari, and R. Shahi. 2011. Weighted cumulative entropy and its estimation. In 2011 IEEE International Conference on Quality and Reliability, 477–80. IEEE.
- [28] Rényi, Alfréd (1961). On measures of information and entropy (PDF). *Proceedings of the fourth Berkeley Symposium on Mathematics, Statistics and Probability 1960*. pp. 547–561.
- [29] Tsallis, C. (1988). Possible generalization of Boltzmann-Gibbs statistics. *Journal of Statistical Physics*. 52 (1–2): 479–487.